ELSEVIER

www.elsevier.nl/locate/carres

Carbohydrate Research 326 (2000) 227–234

CARBOHYDRATE RESEARCH

Molecular dynamics simulations of cyclohenicosakis-[(1→2)-β-D-*gluco*-henicosapyranosyl], a cyclic (1→2)-β-D-glucan (a 'cyclosophoraose') of DP 21

Yong-Hoon Choi [a], Chul-Hak Yang [a], Hyun-Won Kim [b], Seunho Jung [c,*]

[a] *Department of Chemistry, Seoul National University, Seoul 151-742, South Korea*
[b] *Department of Biochemistry, Yonsei University Wonju College of Medicine, Wonju 220-701, South Korea*
[c] *Department of Microbial Engineering, Konkuk University, Mojindong 93-1, Kwangjin-ku, Seoul 143-701, South Korea*

Received 20 September 1999; accepted 1 February 2000

Abstract

We report molecular dynamics simulations of cyclohenicosakis-[(1→2)-β-D-*gluco*-henicosapyranosyl], termed 'cyclosophohenicosamer', a member of a class of cyclic (1→2)-β-D-glucans ('cyclosophoraoses'). Our goals were to provide insights into the conformational preferences of these cyclosophoraoses. Simulated annealing and constant-temperature molecular dynamics calculations were performed on the DP 21 cyclosophohenicosamer. The radius of gyration (R_G) of the molecule and the conformation of glycosidic dihedral angles were used to analyze the result of computational studies. Most glycosidic linkages were concentrated in the lowest-energy region of the $\phi-\psi$ energy map, and the values of radius of gyration from our simulations were consistent with the reported experimental value. The simulations produced various types of compact and asymmetric conformations within reasonable ranges of the glycosidic linkage conformation and radius of gyration. The results indicate the presence of a high degree of molecular flexibility of cyclosophohenicosamer and suggest the uniqueness of inclusion complexation with other molecules through this molecular flexibility.

Keywords: Cyclic (1→2)-β-D-glucan; Cyclosophoraose; Molecular dynamics; Simulated annealing; Conformation

1. Introduction

Cyclic (1→2)-β-D-glucans (known as 'cyclosophoraoses') are a class of unbranched cyclic (1→2)-β-D-glucans produced by Gram-negative bacteria of the genera *Agrobacterium* and *Rhizobium*. These compounds vary in size from 17 to 40 glucosyl units [1,2]. Cyclosophoraoses are known to play an important role in the regulation of osmotic pressure [3,4] and are involved in the initial stage of root-nodule formation of *Rhizobium* during nitrogen fixation [2]. In this process, cyclosophoraoses are suspected to be involved in complexation with various plant flavonoids.

Since the first discovery of cyclosophoraoses, much attention has been focused on their biological functions [5,6], conformations [7,8], and potential ability to form inclusion complexes with other molecules [9–11]. Although the significance of the cyclic structure of cyclosophoraoses is not clearly understood, cyclosophoraoses present a challenge in understanding the relationship

* Corresponding author. Tel.: +82-2-4503520; fax: +82-2-4503520.
E-mail address: shjung@kkucc.konkuk.ac.kr (S. Jung)

0008-6215/00/$ - see front matter
PII: S0008-6215(00)00050-1

between their conformations and physicochemical properties.

The conformation of cyclosophoraoses is important to study biological functions and to develop technological applications. Many experimental and theoretical attempts have been tried to solve this problem. Palleschi and Crescenzi [7] have proposed a symmetrical model for cyclosophoraoses based on the idea of triglucosyl repeat units with a large central cavity. Other researchers have reported more compact conformations of cyclosophoraoses with repeating units [8] or without repeating units [2].

In the present study, we performed molecular dynamics (MD) simulations on a member of the class of cyclosophoraoses composed of 21 β-D-glucosyl units, namely cyclohenicosakis-[(1→2)-β-D-*gluco*-henicosapyranosyl] (termed the 'cyclosophohenicosamer'). We have investigated overall conformational characteristics and the patterns of glycosidic dihedral angles of the compound.

2. Methods

Molecular models and force field.—Molecular modeling calculations were performed with the InsightII/Discover program (version 97.0, Molecular Simulations Inc. San Diego, USA). We used the consistent valence force field (CVFF) [12] with the following representation of potential energy:

$$V(r^N) = \sum_{\text{bonds}} \frac{k_i}{2}(l_i - l_{i,0}) + \sum_{\text{angles}} \frac{k_i}{2}(\theta_i - \theta_{i,0})^2 + \sum_{\text{torsions}} \frac{V_n}{2}(1 + \cos(n\omega - \gamma)) + \sum_{i=1}^{N}\sum_{j=i+1}^{N}\left(4\varepsilon\left[\left(\frac{\sigma_{ij}}{r_{ij}}\right)^{12} - \left(\frac{\sigma_{ij}}{r_{ij}}\right)^{6}\right] + \frac{q_i q_j}{4\pi\varepsilon_0 r_{ij}}\right) \quad (1)$$

The first three terms of Eq. (1) represent the energy of deformation of bond length, the bond angles, and the dihedral angles, respectively. The final term accounts for the van der Waals and electrostatic interactions.

As the three-dimensional structures of cyclosophoraoses are not available, we used a model proposed by Palleschi and Crescenzi [7] for the initial conformation of our simulations. Referring to this paper, a molecular model of cyclosophohenicosamer was built using β-D-glucose from the standard sugar library of the biopolymer module of the InsightII program. This molecule was chosen because of the medium size among the family of cyclosophoraoses [13]. The ϕ and ψ glycosidic dihedral angles were defined as ϕ = (H-1–C-1–O-1–C-2) and ψ = (C-1–O-1–C-2–H-2).

Generation of a disaccharide conformational map of the (1→2)-β-D-glucan.—A disaccharide conformational map was calculated to investigate the low-energy regions of the glycosidic dihedral angles of cyclosophoraoses. Conformations of β-sophorose (i.e., 2-*O*-β-D-glucopyranosyl-β-D-glucopyranoside) were generated by varying ϕ and ψ dihedral angles through a -180 and 180° grid using a 10° grid step. At each point, energies were calculated after energy minimization with restraints for these two angles, but while allowing the other variables to relax [14].

Simulated annealing molecular dynamics.—Conformational search of the cyclosophohenicosamer was performed by simulated annealing molecular dynamics (SA-MD) [15]. In SA-MD, the temperature was changed between 300 and 1000 K five times at intervals of 50 K. At each temperature, MD simulation was performed for 7.5 ps: 1.5 ps of equilibration phase and 6 ps of production phase. One structure was saved at the end of each production phase at 300 K. Total MD simulation time was 1057.5 ps. No cut-off was imposed on the calculation of non-bonded interactions. Constant NVT MD calculations were performed using the leap-frog algorithm with a 1 fs time step. The temperature was controlled by velocity scaling in equilibration phases and by the Berendsen algorithm [16] in production phases with a coupling constant of 0.2 ps. The dielectric constant was set to 1.

After the SA-MD, the five low-temperature conformations were fully energy minimized; 100 iterations of steepest descent minimization and conjugate gradient minimization until the maximum derivative reached below 0.05 kcal/mol Å.

Molecular dynamics in vacuo.—To investigate molecular motion of cyclosophoheni-

cosamer at room temperature, molecular dynamics simulation of cyclosophohenicosamer at 300 K was performed in vacuo. The system was equilibrated for 100 ps and a production run was carried out for 1000 ps. Intermediate structures were saved every 0.25 ps for analysis. Other MD procedures were same as the SA-MD.

Molecular dynamics in water environment.—Cyclosophohenicosamer was solvated with a sphere of 20 Å radius of SPC [17] water molecules ($\sim$920 water molecules). The solvated cyclosophohenicosamer was energy minimized and a preliminary MD simulation was performed with position restraining on the cyclosophoraose for 50 ps to allow further relaxation of the solvent molecules. Subsequently, the production MD simulation was done for 1000 ps. The MD calculations were performed using the Velocity Verlet algorithm [18] at constant volume at 300 K. Nonbonded interactions were calculated by the fast multipole method [19] implemented in the DISCOVERY program. By constraining bond lengths (rattle algorithm) [20], a time step of 2 fs could be used. The temperature was controlled using weak coupling to a bath of constant temperature ($T = 300$ K, $\tau = 0.1443$ ps). The dielectric constant was set to 1. Intermediate structures were saved every 0.25 ps for analysis.

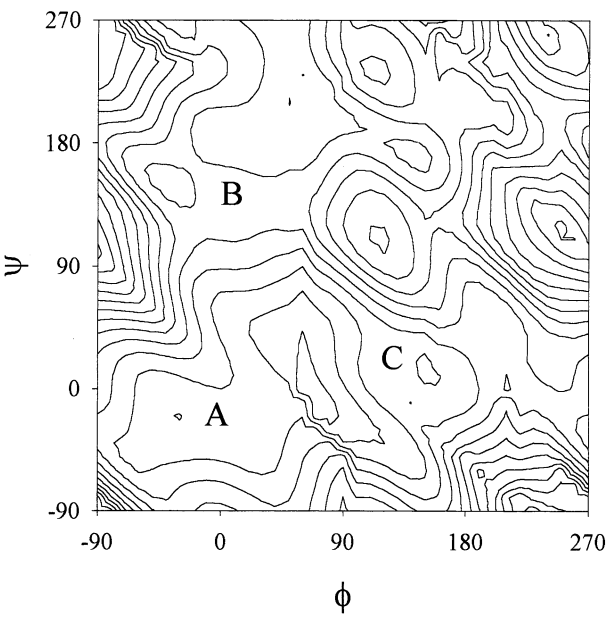

Fig. 1. The ϕ–ψ potential-energy map of β-sophorose dimer. The low-energy regions are specified A, B, and C regions. The contour line corresponds to 2 kcal/mol.

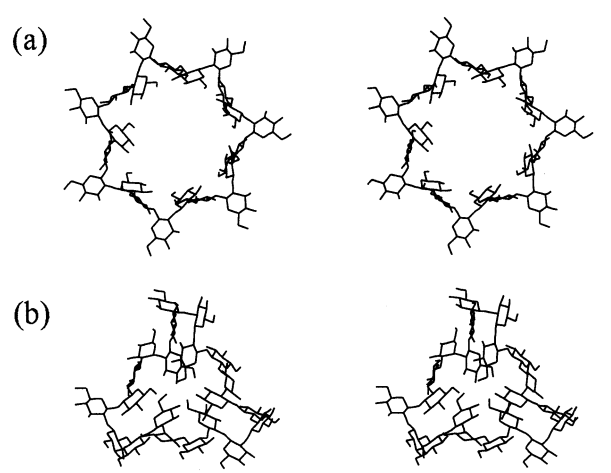

Fig. 2. Stereoview of proposed conformations of cyclosophohenicosamer: (a) proposed by Palleschi and Crescenzi [7]; (b) proposed by York et al. [8]

3. Results

Potential-energy map of β-sophorose.—In Fig. 1, the ϕ–ψ potential-energy map of β-sophorose is shown. This energy contour shows three major low-energy regions, having a centroid at (ϕ, ψ) values of approximately (60°, 10°) for the A-type conformational region, (40°, −170°) for the B-type conformational region, and (−170°, 10°) for the C-type conformational region. The A-type region has the lowest potential energy, and the B- and C-type regions have approximately 8 kcal/mol higher energies than the A-type region.

Simulated annealing molecular dynamics.—Fig. 2 shows the models of cyclosophohenicosamer proposed by Palleschi and Crescenzi [7] and York et al. [8], and Fig. 3 shows the five low-temperature conformers from SA-MD. The overall conformations look quite dissimilar. The root-mean-square displacement (RMSD) between the conformers is approximately in the range of $\sim$6–8 Å, indicating that large conformational space was covered during the SA-MD.

The radius of gyration (R_G) of cyclosophohenicosamer is a good indicator for the evaluation of simulations. The R_G of the five conformers ranged from 8.2 to 9.2 Å with an average value of 8.7 Å, which is close to the

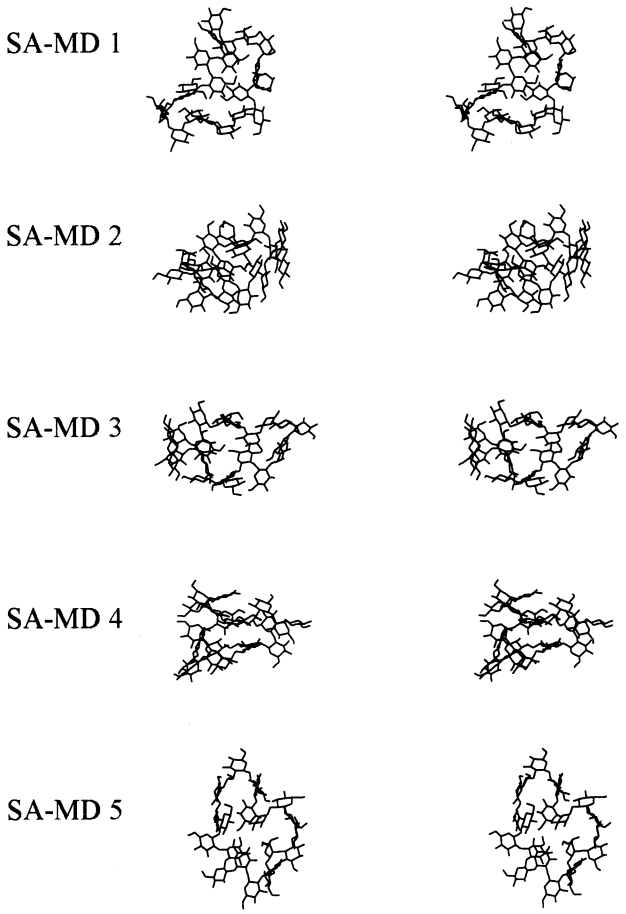

Fig. 3. Stereoview of five low-temperature conformers from SA-MD. Each conformation was saved from each production phase at 300 K.

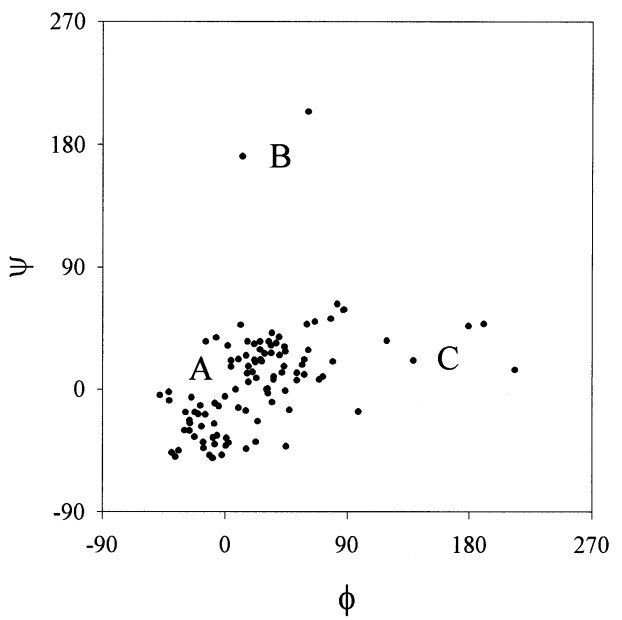

Fig. 4. Ramachandran-like conformational map of $\phi-\psi$ glycosidic dihedral angles, generated for all the glycosidic dihedral angles of the five conformers from SA-MD.

reported value of 8.6 Å, measured by small-angle X-ray scattering (SAXS) [21].

In Fig. 4, in order to explore the conformational patterns, a Ramachandran-like conformational map of glycosidic dihedral angles, ϕ and ψ, was generated for all the glycosidic dihedral angles of the five conformers. The Ramachandran map shows that most of the glycosidic dihedral angles adopt the A-type conformation, which was positioned in the lowest-energy region of the potential-energy map.

In Table 1, the overall conformation of each conformer from SA-MD was expressed in terms of the type of glycosidic dihedral angles. For each conformer, most of the glycosidic conformations adopted the most stable A-type conformation, and one or two dihedral conformations per conformer adopted the less stable B- or C-type conformations.

Molecular dynamics at 300 K in vacuo.— The time change of R_G during the production phase of MD simulation in vacuo is shown in Fig. 5. The 100 ps equilibration phase is not shown. The value of R_G fluctuated around an average value of 8.3 Å, which was similar to the experimental value of 8.6 Å. This value of R_G indicates compact conformations during the MD simulation at 300 K as in SA-MD.

We constructed a population density map as a function of dihedral angles (ϕ, ψ) by counting occurrence in a $10 \times 10°$ angular space for each glycosidic linkage. Fig. 6 shows the two-dimensional (ϕ, ψ) population density map of the glycosidic dihedral angles. The conformations of glycosidic linkages were concentrated in the low-energy regions. The most prevalent glycosidic linkage was the A-type conformation, and relatively small numbers of linkages adopted the B and C conformations, as expected. In Table 1, the general conformation of the cyclosophohenicosamer in this MD simulation was represented in terms of A-, B-, and C-type conformations. A representative conformation from this MD simulation is shown in Fig. 7, and other conformers in this MD simulation were not significantly different from it.

The RMSD between the conformations for the non-hydrogen atoms in this simulation was of order of 2 Å, indicating that limited

conformational space was searched at 300 K and nanosecond time scale. Nevertheless, the conformations obtained here are reasonable on the basis of R_G and the patterns of glycosidic dihedral linkages.

Molecular dynamics at 300 K in a water environment.—The time change of the R_G during the MD simulation of cyclosophoraose in water environment is shown in Fig. 8. R_G decreased during the initial 200 ps, which we regarded as equilibration and thus discarded. During the last 800 ps, which we have used for the analysis reported below, R_G settled into oscillation around an average value of 8.5 Å, which is very similar to the experimental value of 8.6 Å. The presence of water molecules would help to reproduce a more accurate value of R_G compared with simulations in vacuo. The contraction of cyclosophohenicosamer during the MD simulation,

Table 1
Conformation of each conformer from SA-MD, MD in vacuo and in water environment, expressed in terms of the type of glycosidic dihedral angles

Conformation	Distribution of A, B and C-type
SA-MD 1	AAACBAAAAAAAAAAAAAAA
SA-MD 2	AAAAAAAAAAACAAAAAAAA
SA-MD 3	BAAAAAAAAAAAAAAAAAAA
SA-MD 4	AAAAAAAAAAAAAAAAAAAA
SA-MD 5	AAAAAAACAAAAAAAAAAAA
MD in vacuo	AAAAAAAAAAAAAAAAACCA
MD in aq environment	AAAAAABAAAAAAAAAAAAC

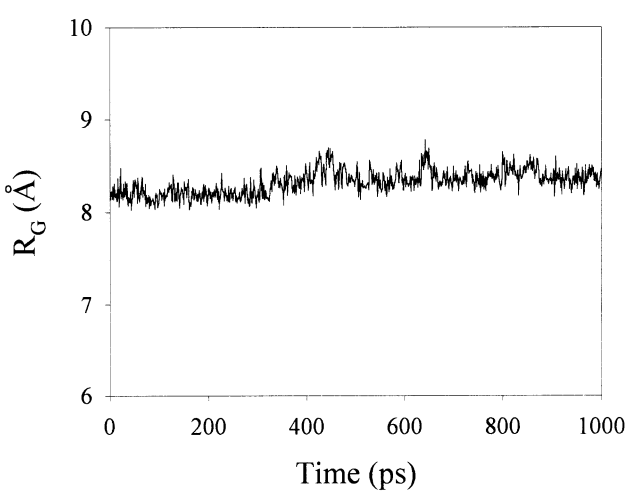

Fig. 5. Time change of R_G during the production phase of the MD simulation in vacuo.

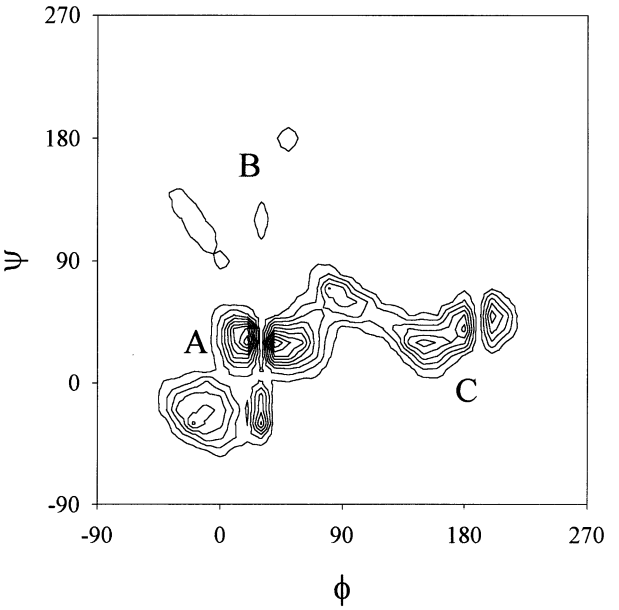

Fig. 6. The $\phi-\psi$ population density map of the glycosidic dihedral angles from the MD simulation in vacuo.

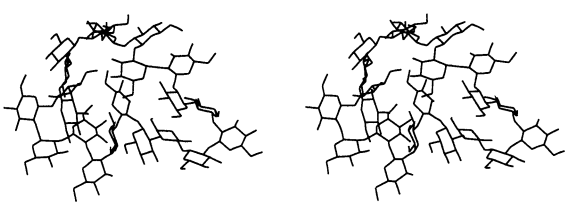

Fig. 7. Stereoview of a representative conformation from the MD simulation in vacuo.

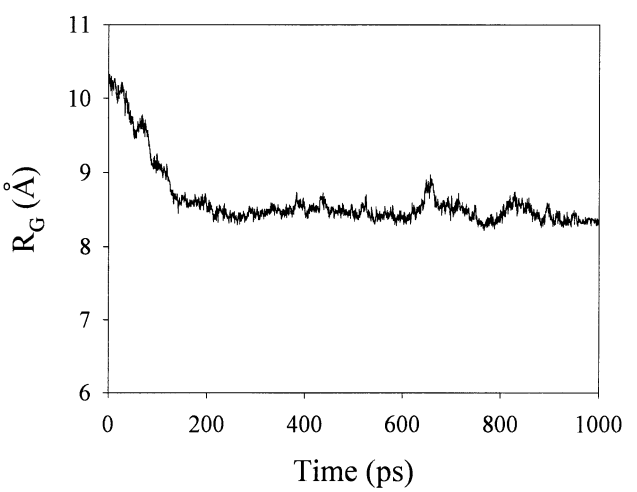

Fig. 8. Time change of R_G during the production phase of the MD simulation in an aqueous environment.

represented by a decrease in R_G, indicates compact conformations during the simulation as in SA-MD and MD at 300 K in vacuo.

A population density map was constructed as above. Fig. 9 shows the two-dimensional (ϕ, ψ) population density map of the glycosidic dihedral angles. The general shape of the map was similar with that of the MD simulations in vacuo. The A-type conformations occupied 91.1%, the B-type conformations occupied 4.8%, and the C-type conformations occupied 4.1% of the population. In Table 1, the overall conformation of the cyclosophohenicosamer in the MD simulation was represented in terms of the A-, B-, and C-type conformations of glycosidic linkages. A representative conformation from this MD simulation is shown in Fig. 10, and other conformers in this simulation were not much different from it.

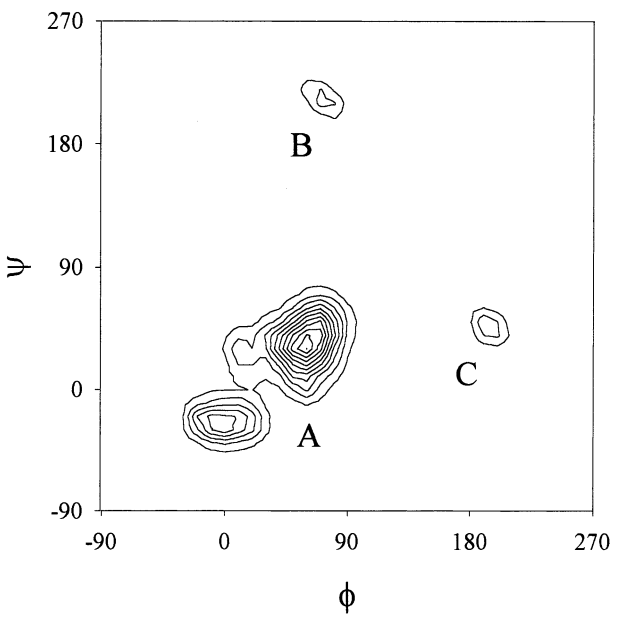

Fig. 9. The $\phi-\psi$ population density map of the glycosidic dihedral angles from the MD simulation in aqueous environment.

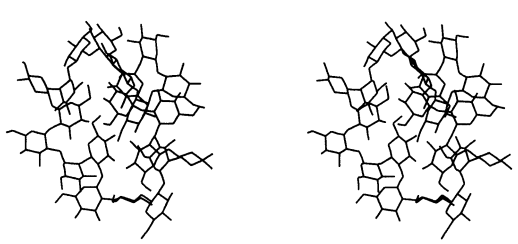

Fig. 10. A representative conformation from the MD simulation in an aqueous environment.

The RMSD between the conformations for the non-hydrogen atoms in this simulation was of order of 2 Å. The position of conformation B and C did not change along the backbone. This indicates that limited conformational space was searched at 300 K and nanosecond time scale in an aqueous environment as in vacuo. Nevertheless, the conformations obtained here were reasonable on the basis of R_G and the patterns of the glycosidic dihedral linkages.

4. Discussion

The $\phi-\psi$ potential energy map and population density map of glycosidic dihedral angles showed favored conformational regions similar to that reported by Mimura et al. [21] and York et al. [8] for sophorose from the rigid-residue Monte Carlo sampling analysis. The map is comparable with the relaxed-residue sophorose model by Dowd et al. [22], who used an MM3 potential function. Also, the lowest-energy A-type conformation is consistent with the conformation of the crystalline form of sophorose hydrate [23]. Throughout the simulations, the $^4C_1$ ring form predominated for glucosyl moieties, as expected [23].

The molecular model of cyclosophohenicosamer of Palleschi and Crescenzi [7] was chosen as the initial conformation of our simulations. We did several trial MD runs and found that this model could produce many different avenues for various conformers, and thus would be adequate for the starting point of conformational searches.

We compared representative conformations from our simulation with structures similar to those reported by Palleschi and Crescenzi [7] and York et al. [8]. The conformations from our simulations were generally more compact than those of Palleschi and Crescenzi and York et al., as indicated by the R_G values. The values of R_G from our simulations were close to the reported value of R_G measured by SAXS in aqueous solution [21], thus validating our results. Table 2 shows the values of R_G and energies after minimization of the conformers of cyclosophohenicosamer.

The conformations from our simulations were generally irregular, as reported by

Table 2
Values of R_G and potential energies after minimization of the conformers of cyclosophohenicosamer [a]

Conformation	R_G (Å)	E_{pot} in CVFF after minimization (kcal/mol)
SA-MD 1	9.2	405.7
SA-MD 2	8.3	386.7
SA-MD 3	9.1	412.6
SA-MD 4	8.2	371.0
SA-MD 5	8.7	437.2
MD in vacuo	8.3	
MD in aq environment	8.5	437.9
Palleschi and Crescenzi [a]	10.2	
York et al. [b]	9.0	
SAXS data	8.6	

[a] Ref. [7].
[b] Ref. [8].

Mimura et al. [21]. We could not find any conformational repeats that could produce symmetric conformations in the course of our simulations. Considering the compactness of the cyclosophohenicosamer, we think that the presence of any repeating units along the backbone could be hardly feasible. Also our simulations produced a variety of conformations. Although the differences in the energies between the conformations after energy minimizations were in the range of 60 kcal/mol, we believe that all the conformations reported here reflect the conformational ensemble of cyclosophohenicosamer. Generally, lower-energy conformers have lower values of R_G, namely, a more compact shape. The compactness of the cyclosophohenicosamer means the abundance of intramolecular hydrogen bonds. In the MD simulations in vacuo, there were an average of 30 intramolecular hydrogen bonds in the MD trajectory. However, in the MD simulation in water, there were an average of 23 intramolecular hydrogen bonds in the MD trajectory. That is the more compact conformations have generally more intramolecular hydrogen bonds, thus lower energies. In an aqueous environment, the number of intramolecular hydrogen bonds decreases by formation of the solvent–solute hydrogen bonds. The R_G values of conformations from the MD in water are closer to that from SAXS experiment than those from MD in vacuo. Considering the value of R_G and the limitations of force field based simulations, we propose that the conformation of the cyclosophohenicosamer is irregular and takes various forms.

Our simulations produced compact conformations with a very small central cavity. Mimura et al. [21], who also reported compact conformations of cyclosophoraoses, suggested that the cavity in a cyclosophoraose might be too small to form an inclusion complex with relatively large molecules. But we have a different opinion. We propose that cyclosophoraoses are very flexible molecules, as shown by relatively large RMSD between conformers from SA-MD and the multiformity of conformations from our simulations. We suggest that cyclosophoraoses can accommodate hydrophobic molecules inside the ring by an 'induced-fit' mechanism, not by a 'lock-and-key' mechanism, as many enzyme–substrate binding mechanisms. Some experimental evidence for the ability of cyclosophoraoses to form inclusion complexes with other molecules was also reported [9,13].

In this study, MD simulations were exploited to provide insight on the conformational features of the 21-unit cyclosophohenicosamer. This approach produced various types of compact and irregular conformations. We suggest that the cyclosophohenicosamer is a highly flexible molecule with no single dominant conformation. Nonetheless, all the conformations from our simulations had a reasonable range of R_G values compared with that of the SAXS experiment. Also, most glycosidic linkages adopted the most stable A-type conformations, as pointed out by other researchers. We suggest that this high molecular flexibility of cyclosophohenicosamer could provide the unique ability for the molecule to form inclusion complexes with other molecules.

Acknowledgements

This work was supported by a grant from Konkuk University in 1999.

References

[1] R.A. Dedonder, W.Z. Hassid, *Biochim. Biophys. Acta*, 90 (1964) 239–247.

[2] I. André, K. Mazeau, F.R. Taravel, I. Tvaroska, *Int. J. Macromol.*, 17 (1995) 189–198.
[3] K.J. Miller, E.P. Kennedy, V.N. Reinhold, *Science*, 231 (1986) 48–51.
[4] A. Dell, W.S. York, M. McNeil, A.G. Darvill, P. Albersheim, *Carbohydr. Res.*, 117 (1983) 185–200.
[5] J.L. Botsford, T.A. Lewis, *Appl. Environ. Microbiol.*, 56 (1990) 488–494.
[6] T. Dylan, D.R. Helinski, G.S. Ditta, *J. Bacteriol.*, 172 (1990) 2400–2408.
[7] A. Palleschi, V. Crescenzi, *Gazz. Chim. Ital.*, 115 (1985) 243–245.
[8] W.S. York, J.U. Thomsen, B. Meyer, *Carbohydr. Res.*, 248 (1993) 55–80.
[9] Y. Okada, S. Horiyama, K. Koizumi, *Yakugaku Zasshi*, 106 (1986) 240–247.
[10] M. Hisamatsu, A. Amemura, T. Matsuo, H. Matsuda, T. Harada, *J. Gen. Microbiol.*, 128 (1982) 1873–1881.
[11] K. Koizumi, Y. Okada, S. Horiyama, T. Utamura, T. Higashiura, M. Ikeda, *J. Incl. Phenom.*, 2 (1984) 891–899.
[12] P. Dauber-Osguthorpe, V.A. Roberts, D.J. Osguthorpe, J. Wolff, M. Genest, A.T. Hagler, *Proteins: Struct. Funct. Genet.*, 4 (1988) 31–47.
[13] C. Kwon, Y.-H. Choi, N. Kim, J.-S. Yoo, C.-H. Yang, H.-W. Kim, S. Jung, *J. Incl. Phenom.*, 36 (2000) 55–64.
[14] C.A. Stortz, *Carbohydr. Res.*, 322 (1999) 77–86.
[15] Y.-H. Choi, S. Kang, C.-H. Yang, H.-W. Kim, S. Jung, *Bull. Korean Chem. Soc.*, 20 (1999) 753–756.
[16] H.J.C. Berendsen, J.P.M. Postma, W.F. van Gunsteren, A. DiNola, J.R. Haak, *J. Chem. Phys.*, 81 (1984) 3684–3690.
[17] H.J.C. Berendsen, J.P.M. Postma, W.F. van Gunsteren, J. Hermans, in B. Pullman (Ed.), *Intermolecular Forces*, Reidel, Dordrecht, 1981, pp. 331–342.
[18] W.C. Swope, H.C. Anderson, P.H. Berens, K.R. Wilson, *J. Chem. Phys.*, 76 (1982) 637–649.
[19] H.Q. Ding, N. Karasawa, W.A. Goddard, *J. Chem. Phys.*, 97 (1992) 4309–4318.
[20] H.C. Andersen, *J. Comp. Phys.*, 52 (1983) 24–34.
[21] M. Mimura, S. Kitamura, S. Gotoh, K. Takeo, H. Urakawa, K. Kanjiwara, *Carbohydr. Res.*, 289 (1996) 25–37.
[22] M.K. Dowd, A.D. French, P.J. Reilly, *Carbohydr. Res.*, 233 (1992) 15–34.
[23] P.J. Ohanessian, F. Longchambon, F. Arene, *Acta Crystallogr., Sect. B*, 34 (1978) 3666–3671.